

Technical Report

Constraining friction properties of mature low-stressed faults such as SAF

SCEC Award #19085, PI Nadia Lapusta

1. Summary of the results

A number of observations suggest (section 3) that well-developed, mature faults such as the San Andreas Fault (SAF) are generally “weak,” i.e. operate at low overall levels of shear stress in comparison with what would be expected from Byerlee’s law and numerous laboratory experiments on quasi-static or low-slip-rate friction (e.g., Byerlee, 1978; Dieterich, 1979, 1981; Tullis and Weeks, 1986; Blanpied et al., 1991, 1995; Marone, 1998; Wibberley et al., 2008 and references therein). If typical low-slip-rate friction coefficients of 0.6-0.8 are multiplied by overburden minus hydrostatic pore pressure, ~150 MPa at the representative seismic depth of 8 km, one obtains shear strength values of ~100 MPa. Faults that operate at much lower levels of stress (~10-20 MPa) are called “weak” and their strength is called “low.”

We have been simulating sequences of earthquakes and aseismic slip in different models for “weak” mature faults, aiming to determine which friction and other fault properties in such models are compatible with a range of available observations such as static stress drops of 1-10 MPa, the observed variations of the breakdown energy and radiated energy with the seismic moment, and the absence of wholesale melting in shear zones. Our eventual goal is to establish which among the acceptable models have behaviors specific to the SAF, including seismic quiescence between large events for some SAF segments and paleoseismic data. We have continued to explore earthquake sequences in models of quasi-statically strong but dynamically weak faults which typically result in self-healing pulse-like ruptures in the regime that reproduces 1-10 MPa static stress drops (Lambert et al., 2020). We have also started to focus on seismological observables in models of chronically weak faults, i.e., ones that have either persistently low effective normal stress due to fluid overpressure or low friction coefficients due to special fault-zone materials. We have developed an approximation for the effects of off-fault yielding in our simulations – which reduces sliding rates and shear heating and increases dissipated energy – by imposing a limit on the fault slip rate as suggested by detailed dynamic rupture simulations (Andrews, 2004).

We have found that self-healing pulse-like ruptures radiate more seismic energy than crack-like ruptures with the same static stress drop and potency (Figure 1; Lambert et al., 2020). We have established that the sharper the self-healing pulse – i.e., the shorter the local slip duration relative to the overall event duration – the lower the dynamic fault resistance relative to the average final stress on the fault (i.e., the more significant the stress overshoot), and the higher the radiated energy per moment (Figure 2; Lambert et al., 2020). In fact, the radiated energy per seismic moment can be an order of magnitude higher for the simulated self-healing pulse-like ruptures than the values inferred teleseismically for natural events (Figure 1; Lambert et al., 2020). We have verified these findings from 2D models with 1D faults in selected simulations of 3D models with 2D faults. These findings suggest that either large earthquakes rarely propagate as self-healing pulses or their radiated energy is substantially underestimated. However, we find that the higher ratios of radiated energy to moment from our simulated self-healing pulses are potentially consistent with limited regional estimates from large crustal earthquakes (Figure 1F). Taking the existing estimates for crustal and megathrust earthquakes at their face value potentially suggests different physical conditions and predominant rupture style for large crustal and megathrust earthquakes, with the former being self-healing pulses on statically strong but dynamically weak faults while the latter being crack-like ruptures on persistently weak faults, with additional mild dynamic weakening to achieve the right range of stress drops.

We have also found a parameter regime in which quasi-statically strong but dynamically weak faults operate under low stresses but produce crack-like ruptures rather than self-healing pulses, with radiated energies close to those of natural events (Figure 3). Furthermore, we have established that crack-like and moderately pulse-like ruptures on chronically weak faults with additional relatively mild co-seismic

weakening satisfy both the low-stress, low-heat fault operation and the seismological constraints on stress drop, radiated energy (teleseismic estimates), radiation efficiency, and breakdown energy (Perry et al., 2020; Lambert et al., 2020). Our findings indicate that enhanced dynamic weakening is an important ingredient for reproducing seismological observations; for example, chronically weak fault models with high fluid overpressure require enhanced weakening to produce static stress drops greater than 1 MPa.

2. Relevance of the project goals to the objectives of SCEC

Our project addresses the following SCEC Research Priorities:

P1.c. Constrain how absolute stress and stressing rate vary laterally and with depth on faults

P3.c. Assess how shear resistance and energy dissipation depend on the maturity of the fault system

P1.d. Quantify stress heterogeneity on faults at different spatial scales

P5.a. Develop earthquake simulators that encode the current understanding of earthquake predictability.

Our study will determine which models of low-stresses faults are consistent with basic observations and hence put constraints on the absolute levels of both shear and effective normal stress at all depths, contributing to priority P1.c. Our efforts towards studying the seismological observables and energy budget for all our simulated events will contribute to P3.c. We will study which levels of roughness-motivated heterogeneity on faults is consistent with seismic quiescence observed for several SAF segments, thus contributing to priority P1.d. We will also contribute to P1.d by quantifying the resulting variability of stress before large events. Our goal to produce models of low-stressed SAF segments consistent with basic observations will help towards developing realistic earthquake simulators with predictive power, as in P5.a. The proposed modeling significantly contributes to a number of research priorities of FARM, including “Constrain how absolute stress, fault strength and rheology vary with depth on faults,” and “Determine how seismic and aseismic deformation processes interact.” Confirming that “weak” fault models with low shear stress values are compatible with available observations will contribute to the Community Stress Model.

3. Evidence for “weak” mature faults and two classes of models

The outflow of heat observed for SAF and other mature faults implies that shear stresses acting during sliding are of the order of 10 MPa or less (e.g., Brune et al., 1969; Henyey and Wassenburg, 1971; Lachenbruch and Sass, 1973; Lachenbruch, 1980; Nankali, 2011). Analyses of the fault core obtained by drilling through shallow parts of faults that have experienced major recent events, including the great 2011 Mw 9.0 Tohoku-Oki event, point to co-seismic friction coefficients as low as ~ 0.1 (e.g., Tanikawa and Shimamoto, 2009; Fulton et al., 2013). Low values for shear stresses acting on major faults including SAF are also supported by the inferences of steep angles between the principal stress direction and fault trace (e.g., Townend and Zoback, 2004; Zoback et al., 2007), significant rotations of principal stress directions due to stress drop in earthquakes as judged by the focal mechanisms of microseismicity (e.g., Wesson and Boyd, 2007), geometry of thrust-belt wedges (e.g., Suppe, 2007), and scarcity of pseudotachylytes, the products of solidifying rock melts (e.g., Sibson, 1975; Rice, 2006).

Two classes of models can explain earthquake occurrence under low shear stress. In the first class (Hypothesis 1, H1), the quasi-static friction is high on average, but fault resistance to slip weakens substantially at seismic slip rates as supported by lab experiments (Tullis, 2015 and references therein; Noda et al., 2009; Noda and Lapusta, 2010, 2013; Jiang and Lapusta, 2016). Earthquake rupture initiates in places of stress concentrations and/or statically weak spots and propagates over the rest of the low-stressed fault due to co-seismic weakening, making the fault appear weak. In the second one, the faults are chronically weak (Hypothesis 2, H2), both during slow (quasi-static) and fast (seismic) slip, due to either low friction coefficients, or low effective normal stress, or both. Such models are supported by low quasi-static friction coefficients for some minerals in the lab (although most of them are also rate-strengthening) and observations of fluid overpressure (e.g., Brown et al., 2003; Faulkner et al., 2006; Bellot, 2008; Bangs et al., 2009; Collettini et al., 2009; Fulton and Saffer, 2009; Carpenter et al., 2011; Lockner et al., 2011). Note that fluid overpressure may be confined to the immediate vicinity of the fault

(e.g., Rice, 1992) (and hence not readily observable by bulk velocity studies), due to much higher along-fault permeability compared to the surrounding rock.

While both classes of models can explain fault operation under low shear stress, other aspects of their behavior should exhibit substantial differences. Chronically weak faults operate at the average shear stress levels close to the average quasi-static fault strength (Figure 2C). For the quasi-statically strong but co-seismically weak faults, the average shear stress on the fault is much lower than its average quasi-static strength (Figure 2B). One expected consequence of this difference is in the temporal and spatial patterns of microseismicity occurrence in the two models (e.g., Jiang and Lapusta, 2016; 2017). Another potential difference is in the energy budget and radiation efficiency that we have been studying in our models.

4. Crustal faults and subduction zones may be governed by different physical conditions and rupture styles

Our studies of earthquake sequences (Perry et al., 2020; Lambert et al., 2020) have found that models with mild to moderate enhanced co-seismic weakening due to thermal pressurization of pore fluids result in predominantly crack-like ruptures and require persistently weak fault conditions (e.g., effective normal stresses < 25 MPa) in order to maintain low-stress, low-heat conditions, consistent with hypothesis 2 (Figures 1-2). In contrast, models of quasi-statically strong faults that incorporate more efficient enhanced co-seismic weakening result in low-stress, low-heat fault operation and reasonable stress drops (1-10 MPa), as in hypothesis 1, mainly by producing self-healing pulse-like ruptures (Figure 1A). However, the sharper the self-healing pulse, the larger the stress undershoot that it produces (Figure 2; Lambert et al., 2020), which translates into increasingly larger available energy, in the words of the standard energy analysis. The work of Viesca and Garagash (2015) assumed that this extra energy goes into breakdown energy. However, in our models, much of it is radiated, resulting in the radiated energy to moment ratio from the simulated self-healing pulse-like ruptures being much larger, by nearly an order of magnitude, than the teleseismic seismological inferences for large natural earthquakes (Lambert et al. 2020 and references therein, Figure 1).

This finding implies that (i) either large natural earthquakes rarely propagate as sharp self-healing pulses, or (ii) if such sharper pulse-like ruptures do often occur (e.g. Heaton 1990), then their radiated energy is underestimated by teleseismic methods, by up to an order of magnitude. However, we also find that the higher ratios of radiated energy to moment is consistent with limited regional estimates from large crustal earthquakes (Figure 1F), suggesting that the substantial difference in estimated radiated energy between pulse-like and crack-like rupture models could also indicate differences between large crustal and megathrust earthquakes. These results indicate a need to review the accuracy of radiated energy estimates, especially since regional estimates tend to be higher than the teleseismic ones for the earthquakes for which both are available (Figure 1F).

We have started to verify these conclusions (obtained in 2D models with 1D faults) in 3D models with 2D faults, as in Jiang and Lapusta (2016, 2017). 3D models would also allow us to explore geometric mechanisms of generating slip pulses, due to arrest waves from geometric restrictions of the rupture area such as the seismogenic depth (Day, 1982) or from strong heterogeneities (Beroza and Mikumo, 1996, Michel et al., 2017). A number of assumptions go into estimating radiated energy from seismological recordings; in particular, many seismological studies estimate radiated energy from teleseismic direct p-waves and must apply considerable corrections given that much of the energy is attenuated before arrival (Venkataraman and Kanamori, 2004, Ye et al., 2016 a-c, Kanamori et al., 2019). We are working to produce synthetic waveforms for our simulated 3D sources with different rupture styles, which will allow us to compare the radiated energy computed directly from our models with estimates obtained by applying standard seismological techniques.

6. Including enhanced dynamic weakening is important for matching seismological observations

Even if current teleseismic radiated energy estimates are accurate, which would imply that many large earthquakes do not propagate as self-healing pulses in quasi-statically strong, dynamically weak faults, our models show that enhanced dynamic weakening is still an important ingredient for explaining a range of seismological inferences. For example, enhanced weakening is required to produce static stress drops greater than 1 MPa in persistently weak fault models with chronic near-lithostatic fluid overpressure, since stress changes governed by standard rate-and-state friction only would greatly diminish for low effective normal stress. Our models have demonstrated that persistently weak faults with additional enhanced weakening are capable of reconciling a range of observations, including nearly magnitude-invariant static stress drops, with values consistent with natural earthquakes, and the inferred increase in breakdown energy with slip (Perry et al., 2020). Enhanced weakening for either statically strong or weak faults may explain the seismic quiescence of faults that have historically produced large earthquakes, such as the Carrizo and Cholame segments of the San Andreas Faults (Jiang and Lapusta, 2016).

We have also found a parameter regime in which quasi-statically strong but dynamically weak faults operate under low stresses but produce crack-like ruptures rather than self-healing pulses, with radiated energies and static stress drops close to those of natural events (Figure 3). The main difference between self-healing pulses and very-efficient-weakening crack-like ruptures is that self-healing pulses experience substantial local healing and rapid relocking behind the rupture front, whereas the crack-like ruptures continue to slide at seismic slip rates until the arrival of arrest waves from the rupture boundaries. Note that the radiated energy, average static stress drop and moment may be comparable for crack-like ruptures with mild or extremely efficient weakening (Fig. 1B vs. Fig 3B), however ruptures with more efficient weakening may be potentially distinguished by their production of considerably stronger high-frequency (> 1 Hz) near-fault ground motions (Lambert et al., 2020). The physical plausibility of such theoretically possible very-efficient-weakening crack-like ruptures on natural faults warrants further study, as they require considerably more efficient weakening than the more generic self-healing pulses, and such special weakening may potentially be easily suppressed, for example, by changes in rock permeability or additional energy loss due to off-fault damage during dynamic rupture.

Publications

- Perry, S., Lambert, V. and N. Lapusta (2020). Nearly Magnitude-Invariant Stress Drops in Simulated Crack-Like Earthquake Sequences on Rate-and-State Faults with Thermal Pressurization of Pore Fluids. *J. Geophys. Res. Solid Earth*, doi:10.1029/2019JB018597.
- Lambert, V., Lapusta, N. and S. Perry (2020). Are large earthquakes self-healing pulses or mild cracks? In review.
- Lambert, V. and N. Lapusta (2020). Comparison of seismological techniques for estimating radiated energy from crack-like ruptures and self-healing pulses. In preparation.

Presentations

- Lambert, V. and N. Lapusta. Constraining physical conditions for the low-stress, low-heat operation of mature faults (oral presentation), SCEC workshop on co-seismic fault friction, Pomona, Jan. 2020.
- Lambert, V. and N. Lapusta. Combining kinematic and energetic inferences to constrain physical conditions for the low-stress, low-heat operation of mature faults (Poster presentation), AGU Fall Meeting, San Francisco, CA, Dec. 2019.
- Lambert, V. and N. Lapusta. Modeling the low-stress, low-heat operation of mature faults. (Poster presentation) SCEC Annual Meeting, Palm Springs, CA. 2019.
- Lambert, V. and N. Lapusta. Energy budget of earthquakes: connecting remote observations with local physical behavior (Oral presentation), Numerical Modeling of Earthquake Motions, Smolenice, Slovakia, July. 2019.
- Lambert, V. and N. Lapusta. Energy budget of dynamic shear ruptures: connecting remote observations with local physical behavior (Poster presentation), Engineering Mechanics Institute, Pasadena, CA, June, 2019.

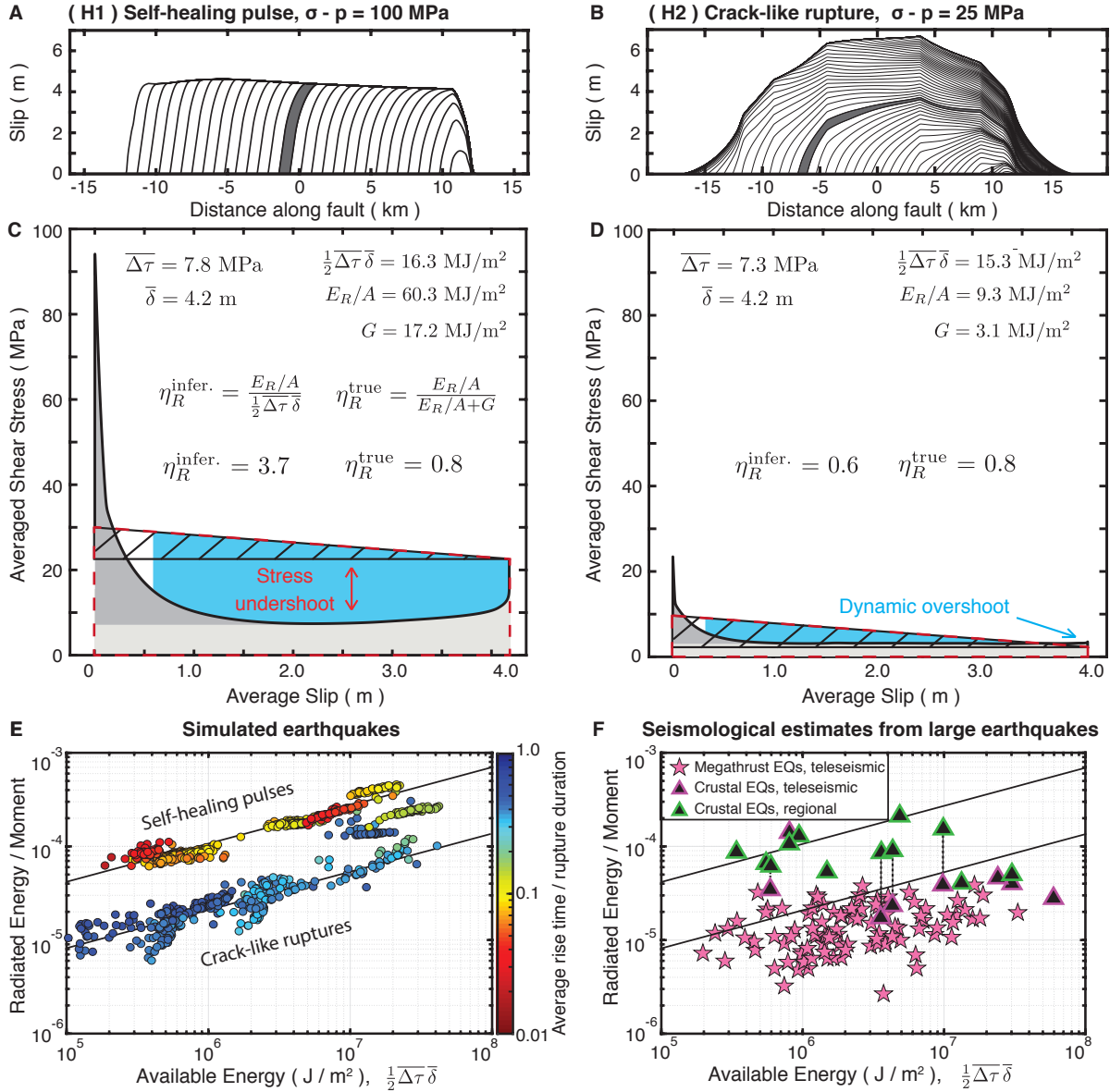


Figure 1: Radiated energy per moment is much higher for self-healing pulses on quasi-statically strong but dynamically weak faults than for crack-like ruptures on chronically weak faults, with potential correspondence to crustal and megathrust faults, respectively. (A-B) Slip evolution for a self-healing pulse and crack-like ruptures with similar average static stress drop and slip (contours every 0.25 s). (C-D) The corresponding average evolution of shear stress vs. slip which also illustrates the energy budget, with the total strain energy change (dashed red trapezoid) partitioned into radiated energy (blue shading) and dissipated energy (gray shading). The self-healing pulse experiences substantial stress undershoot. (E-F) The radiated energy to moment ratio for simulated self-healing pulses (yellow to red colors) is much larger than inferred for megathrust earthquakes from teleseismic measurements (pink stars) but consistent with limited regional estimates from large crustal earthquakes (green triangles). The radiated energy to moment ratio for simulated crack-like ruptures (bluish colors) is comparable to teleseismic inferences for megathrust earthquakes. Note that the accuracy of radiated energy estimates needs to be further evaluated, since different methods provide different estimates; dashed lines connect teleseismic and regional estimates for the same earthquake, where available. From Lambert et al. (2020).

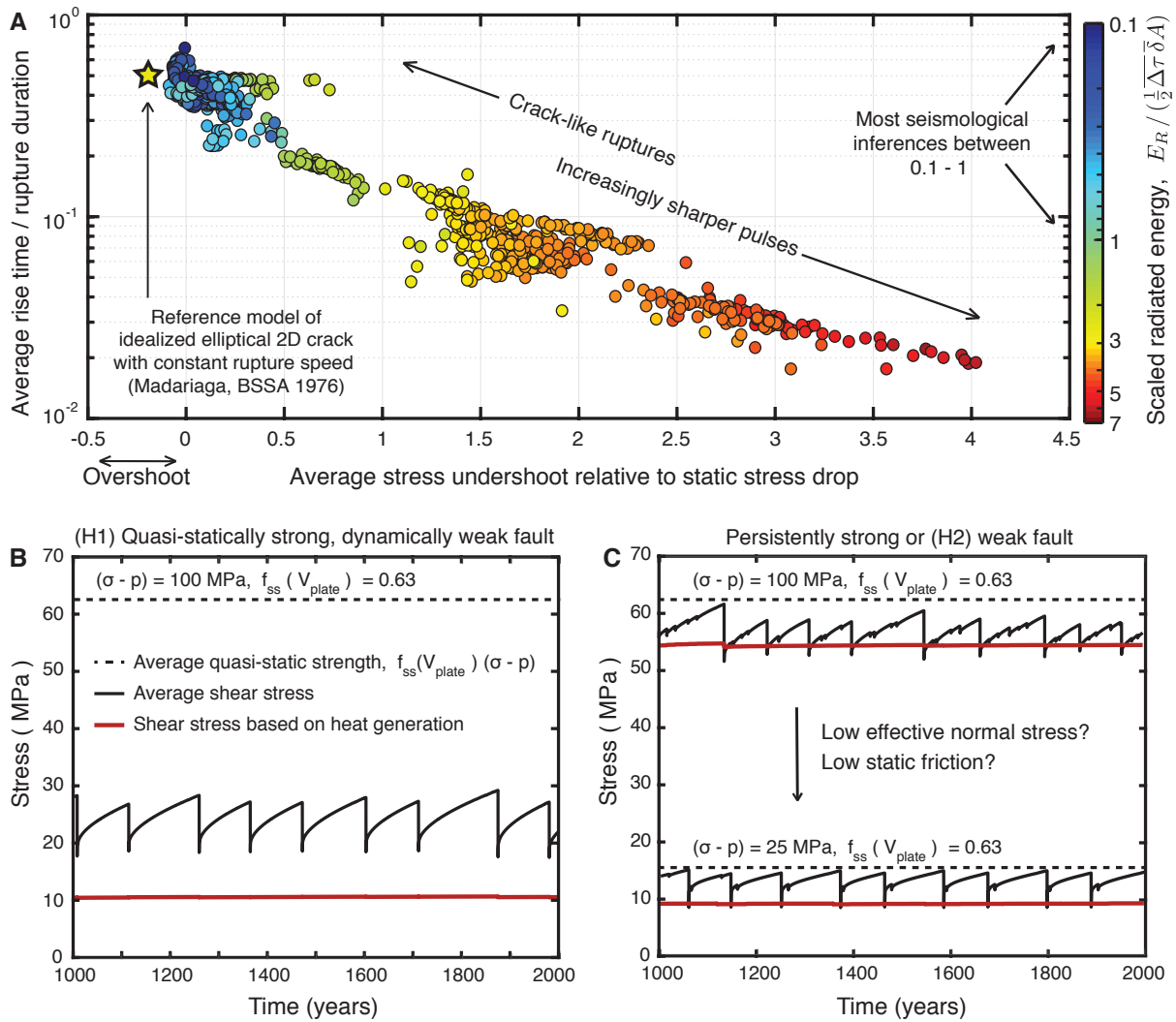


Figure 2: (A) Progressively sharper self-healing pulses, with shorter local slip durations compared to total rupture duration, experience larger average stress undershoots and, as a consequence, result in more radiated energy for the same static stress drop and moment. (B-C) The evolution of average shear stress and shear heating stress over sequences of ruptures simulated on a quasi-statically strong but dynamically weak fault (B) and a persistently weak/strong fault (C). The average shear stress is far from the quasi-static strength in the former case but comparable to it in the latter case. From Lambert et al. (2020).

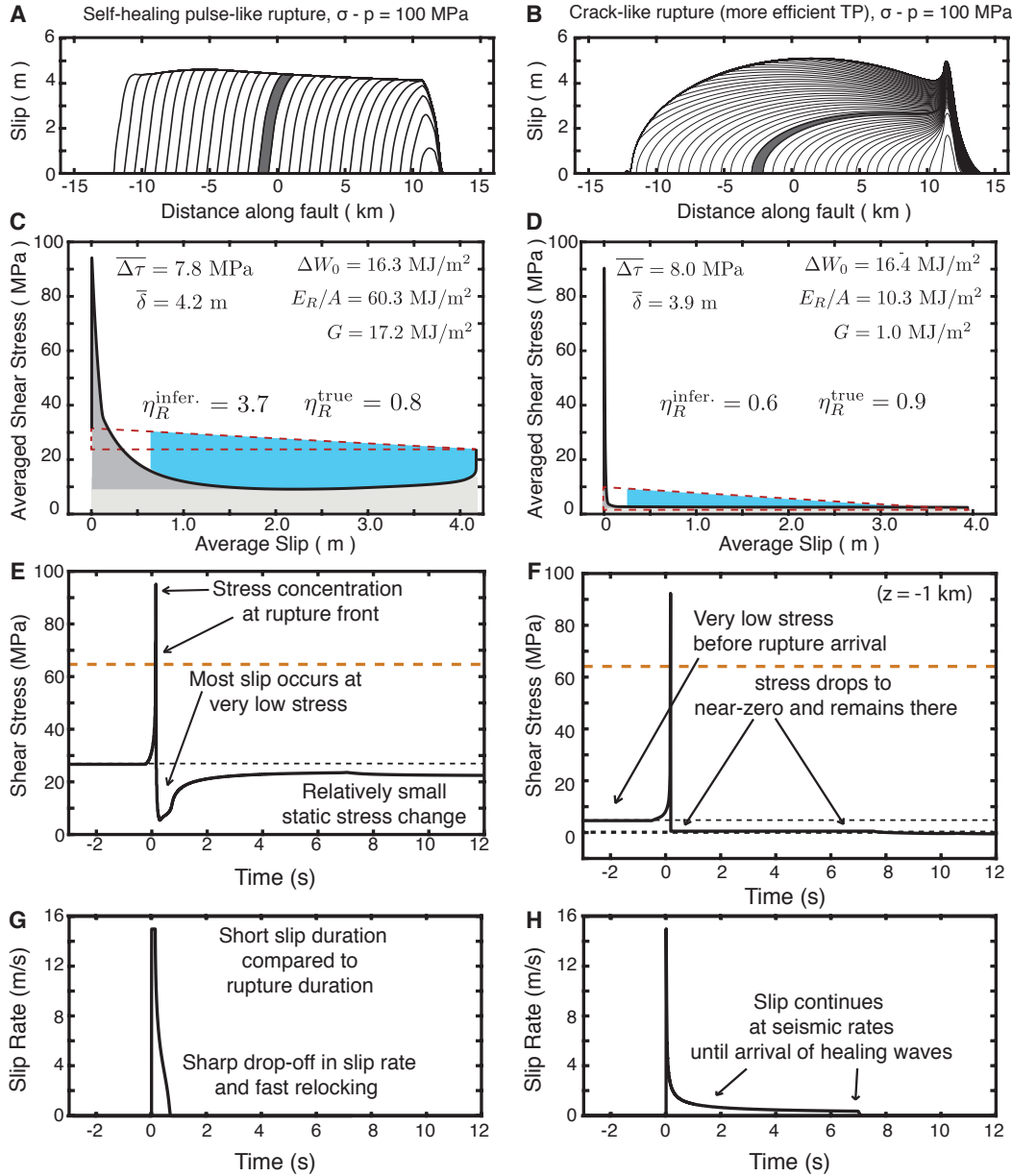


Figure 3: (A-B) Evolution of slip along the fault for a self-healing pulse-like rupture (A) and crack-like rupture (B) with more efficient enhanced weakening. Contours are plotted every 0.25 s. (C-D) The corresponding average evolution of shear stress vs. slip. The seismologically-inferable available energy (red-dashed triangle) illustrates that the two ruptures have similar static stress drop and average slip, however the radiated energy (blue shading) is considerably larger for the self-healing pulse. (E-F) Local evolution of shear stress with time at a point ($z = -1$ km) at the center of the ruptures. Both points have initially low prestress, well below the local quasi-static strength (orange dashed line), before the arrival of the stress concentration at the rupture front. The self-healing pulse dramatically weakens and then heals such that the static stress change is much smaller than the dynamic stress change. In contrast, the shear stress within the crack-like rupture drops and stays low, resulting in comparable local static and dynamic stress drops. (G-H) Evolution of slip rate with time at the same points. Local sliding is very short in the self-healing pulse-like rupture before the point quickly relocks, whereas the point continues to slip with seismic slip rates (~ 1 m/s) until the arrival of healing waves from the boundary in the crack-like rupture. Adapted from Lambert et al. (2020).

References

- Abercrombie, R. E., and J. R. Rice (2005), Can Observations of earthquake scaling constrain slip weakening? *Geophys. J. Int.*, 162, 406-424, doi: 10.1111/j.1365-246X.2005.02579.x.
- Abercrombie, R. E. (2014), Stress drops of repeating earthquakes on the San Andreas Fault at Parkfield, *Geophys. Res. Lett.*, 41, 8784–8791, doi:10.1002/2014GL062079.
- Abercrombie, R. E., S. Bannister, J. Ristau, and D. Doser (2017), Variability of earthquake stress drop in a subduction setting, the Hikurangi Margin, New Zealand, *Geophys. J. Int.*, 208, 306-320, doi: 10.1093/gji/ggw393.
- Allmann, B.P., and P.M.Shearer (2007), Spatial and temporal stress drop variations in small earthquakes near Parkfield, California, *J. Geophys. Res.*, 112, B04305, doi: 10.1029/2006JB004395.
- Allmann, B.P., and P.M.Shearer (2009), Global variations of stress drop for moderate to large earthquakes, *J. Geophys. Res.*, 114, B01310, doi:10.1029/2008JB005821.
- Baltay, A., S. Ide, G. Prieto, and G. Beroza (2011), Variability in earthquake stress drop and apparent stress. *Geophys. Research Letters.*, 38, L06303, doi:10.1029/2011GL046698.
- Bangs N.L.B., G.F. Moore, S.P.S. Gulick, E.M. Pangborn, H.J. Tobin, S. Kuramoto, and A. Taira, Broad (2009), weak regions of the Nankai Megathrust and implications for shallow coseismic slip, *Earth. Planet. Sci. Lett.*, 284, 44-49.
- Bellot, J. P. (2008), Hydrothermal fluids assisted crustal-scale strike-slip on the Argentat fault zone, *Tectonophysics*, 450, 21-33.
- Beroza, G. C., and H. Kanamori (2007), Earthquake Seismology: Comprehensive Overview, *Treatise on Geophysics*, Volume 4: Earthquake Seismology, 9. 1-58, edited by G. Schubert, Elsevier.
- Blanpied, M. L., D. A. Lockner, and J. D. Byerlee (1991), Fault stability inferred from granite sliding experiments at hydrothermal conditions, *Geophys. Res. Letters*, 18(4), 609-612.
- Blanpied, M. L., D. A. Lockner and J. D. Byerlee (1995), Frictional slip of granite at hydrothermal conditions, *J. Geophys. Res.*, 100, 13045-13064.
- Brodsky, E. E., J. J. Gilchrist, A. Sagy, and C. Collettini (2011), Faults smooth gradually as a function of slip, *Earth. Planet. Sci. Lett.*, 302(1-2), 185–193, doi:10.1016/j.epsl.2010.12.010.
- Brown, K.M., A. Kopf, M.B. Underwood, and J.L. Weinberger (2003), Compositional and fluid pressure controls on the state of stress on the Nankai subduction thrust: A weak plate boundary, *Earth. Planet. Sci. Lett.*, 214, 589-603.
- Brune, J. N., T. L. Henyey, and R. F. Roy, Heat Flow (1969), Stress, and Rate of Slip along the San Andreas Fault, California, *J. Geophys. Res.*, 74(15), 3821–3827.
- Brune, J. (1970), Tectonic stress and the spectra of seismic shear waves from earthquakes, *J. Geophys. Res.*, 75, 4997–5009, doi:10.1029/JB075i026p04997.
- Brune, J. N. (1971), Correction, *J. Geophys. Res.*, 76, 5002.
- Bydlon, S. A., and E. M. Dunham (2015), Rupture dynamics and ground motions from earthquakes in 2-D heterogeneous media, *Geophysical Research Letters*, 42(6), 1701-1709, doi:10.1002/2014GL062982.
- Byerlee, J. D. (1978), Friction of rocks, *Pure and Applied Geophysics*, 116: 615–626, doi:10.1007/BF00876528.
- Candela, T., F. Renard, M. Bouchon, A. Brouste, D. Marsan, J. Schmittbuhl, and C. Voisin (2009), Characterization of Fault Roughness at Various Scales: Implications of Three-Dimensional High Resolution Topography Measurements, *Pure Appl. Geophys.*, 166(10), 1817–1851.
- Carpenter, B. M., C. Marone, and D. M. Saffer (2011), Weakness of the San Andreas Fault revealed by samples from the active fault zone, *Nature Geosci.*, 4, 251–254.
- Collettini, C., A. Niemeijer, C. Viti, and C. Marone (2009), Fault zone fabric and fault weakness, *Nature*, 462, 907-910.

- Dieterich, J.H. (1979), Modeling of rock friction, 1. Experimental results and constitutive equations, *J. Geophys. Res.*, 84, 2161–2168.
- Dieterich, J.H. (1981), Constitutive properties of faults with simulated gouge, in *Mech. Behavior Crustal Rocks*, edited by N.L. Carter et al., *Geophys. Monogr. Ser.*, 24, 103–120. AGU, Washington, D.C.
- Faulkner D. R., T. M. Mitchell, D. Healy, and M. J. Heap (2006), Slip on 'weak' faults by the rotation of regional stress in the fracture damage zone, *Nature*, 444, 922-925.
- Fulton, P. M. and D. M. Saffer (2009), Potential role of mantle-derived fluids in weakening the San Andreas Fault, *J. Geophys. Res.*, 114, B07408.
- Fulton, P.M., E. E. Brodsky, Y. Kano, J. Mori, F. Chester, T. Ishikawa, R. N. Harris, W. Lin, N. Eguchi, S. Toczko (2013), Expedition 343, 343T, and KR13-08 Scientists, Low Coseismic Friction on the Tohoku-Oki Fault Determined from Temperature Measurements, *Science*, 342, 1214-1217.
- Goebel, T. H. W., E. Hauksson, P. M. Shearer, and J. P. Ampuero (2015), Stress-drop heterogeneity within tectonically complex regions: a case study of San Geronio Pass, southern California, *Geophys. J. Int.*, 202, 514-528, doi: 10.1093/gji/ggv160.
- Hauksson, E., W. Yang, and P. M. Shearer (2012), Waveform Relocated Earthquake Catalog for Southern California (1981 to June 2011), *Bulletin of the Seismological Society of America*, 102(5), 2239–2244, doi:10.1785/0120120010.
- Henye, T. L. and G. J. Wasserburg (1971), Heat Flow near Major Strike-Slip Faults in California, *J. Geophys. Res.*, 76(32), 7924–7946.
- Ide, S. and G. C. Beroza (2001), Does apparent stress vary with earthquake size? *Geophysical Research Letters*, 28(17), 3349-3352.
- Jiang, J. and N. Lapusta (2016), Deeper penetration of large earthquakes on seismically quiescent faults, *Science*, 352, 1293-1297, doi:10.1126/science.aaf1496.
- Jiang, J., and Lapusta, N. (2017), Connecting depth limits of interseismic locking, microseismicity, and large earthquakes in models of long-term fault slip, *J. Geophys. Res.*, doi: 10.1002/2017JB014030.
- Kanamori, H. and D. L. Anderson (1975), Theoretical basis of some empirical relations in seismology, *Bull. Seismol. Soc. Am.*, 65, 1073–1095.
- Kanamori, H. and E. E. Brodsky (2004), The physics of earthquakes, *Rep. Prog. Phys.*, 67, 1429-1496.
- Kanamori, H., L. Ye, B.-S. Huang, H.-H. Huang, S.-J. Lee, W.-T. Liang, Y.-Y. Lin, K.-F. Ma, Y.-M. Wu, and T.-Y. Yeh (2016), A strong-motion hot spot of the 2016 Meinong, Taiwan, earthquake (Mw=6.4), *Terr. Atmos. Oceanic Sci.*, Accepted
- Kaneko, Y. and P. M. Shearer (2014), Seismic source spectra and estimated stress drop derived from cohesive-zone models of circular subshear rupture, *Geophys. J. Int.*, 197, 1002–1015, doi:10.1093/gji/ggu030.
- Kaneko, Y. and P.M. Shearer (2015), Variability of seismic source spectra, estimated stress drop, and radiated energy, derived from cohesive-zone models of symmetrical and asymmetrical circular and elliptical ruptures, *J. Geophys. Res.*, 120, 1053-1079, doi:10.1002/2014JB011642.
- Kita, S., and K. Katsumata (2015), Stress drops for intermediate-depth intraslab earthquakes beneath Hokkaido, northern Japan: Differences between the subducting oceanic crust and mantle events, *Geochem. Geophys. Geosyst.*, 16, 552-562, doi:10.1002/2014GC005603.
- Ko, J. Y.-T., and B.-Y. Kuo (2016), Low radiation efficiency of the intermediate-depth earthquakes in the Japan subduction zone, *Geophys. Res. Lett.*, 43, 11611-11619, doi: 10.1002/2006GL070993.
- Lachenbruch, A.H., and J. H. Sass (1973), Thermo-mechanical aspects of the San Andreas fault system, in Kovach, R L., and Nur, Amos, eds., *Proceedings of the conference on tectonic problems of the San Andreas fault system: Stanford, Calif.*, Stanford University Publications in the Geological Sciences, 13, 190-205.
- Lachenbruch, A. H. (1980), Frictional heating, fluid pressure and the resistance to fault motion, *J. Geophys. Res.*, 85, 6097-6112.

- Lambert, V., Lapusta, N. and S. Perry (2020). Are large earthquake self-healing pulses or mild crack? In review.
- Lee, S.-J., T.-Y. Yeh, and Y.-Y. Lin (2016a). Anomalous strong ground motion in the 2016 Meinong, Taiwan M6.6 earthquake: A synergy effect of source rupture and site amplification, *Seismol. Res. Lett.*, 87(6), doi: 10.1785/0220160082.
- Lee, S.-J., T.-Y. Yeh, T.-C. Lin, Y.-Y. Lin, T.-R.A. Song, and B.-S. Huang (2016b), Two-stage composite megathrust slip of the 2015 MW8.4 Illapel, Chile earthquake, *Geophys. Res. Lett.*, 43, 4979–4985, doi:10.1002/2016GL068843.
- Lin, Y.-Y., K.-F. Ma, and V. Oye (2012), Observation and Scaling of Microearthquakes from Taiwan Chelungpu-fault Borehole Seismometers, *Geophys. J. Int.*, 190, 665–676, doi: 10.1111/j.1365-246X.2012.05513.x.
- Lin, Y.-Y., K.-F. Ma, H. Kanamori, T.-R. A. Song, N. Lapusta, and V. C. Tsai (2016), Evidence for Non-Self-similarity of Microearthquakes Recorded at the Taiwan Borehole Seismometer Array, *Geophys. J. Int.*, 206, 757-773.
- Lin, Y.-Y., T.-Y. Yeh, K.-F. Ma, S.-J. Lee, B.-S. Huang, and Y.-M. Wu (2016), Source complexity of the Meinong Earthquake ML 6.6 2016 in Taiwan, *in preparation*.
- Lin, Y.-Y. and N. Lapusta (2016), Exploring variations of earthquake moment on patches with heterogeneous strength, *AGU annual meeting*.
- Lin, Y.-Y., T.-Y. Yeh, K.-F. Ma, S.-J. Lee, B.-S. Huang, and Y.-M. Wu (2017), Source characteristics of the 2016 Meinong (M_L 6.6), Taiwan, earthquake, revealed from dense seismic arrays: double sources and pulse-like velocity ground motion, *Bull. seism. Soc. Am.*, accepted.
- Lockner, D. A., C. Morrow, D. Moore, and S. Hickman (2011), Low strength of deep San Andreas fault gouge from SAFOD core, *Nature*, 472, 82-85.
- Ma, K.-F., Y.-Y. Lin, S.-J. Lee, J. Mori, and E. E. Brodsky (2012), Evidence on Isotropic Events Observed with a Borehole Array in the Chelungpu Fault Zone, Taiwan, *Science*, 337, 459-463, doi: 10.1126/science.1222119
- Madariaga, R. (1976), Dynamics of an expanding circular crack, *Bull. Seismol. Soc. Am.*, 66, 639–666.
- Marone, C. (1998), Laboratory-derived friction laws and their application to seismic faulting, *Ann. Revs. Earth & Plan. Sci.*, 26, 643-696.
- Nankali, H. R. (2011), Slip rate of the Kazerun Fault and Main Recent Fault (Zagros, Iran) from 3D mechanical modeling, *J. Asian Earth Sci.*, 41, 89-98.
- Noda, H., E. M. Dunham, and J. R. Rice (2009), Earthquake ruptures with thermal weakening and the operation of major faults at low overall stress levels, *J. Geophys. Res.*, **114**, B07302, doi:10.1029/2008JB006143.
- Noda, H. and N. Lapusta (2010), Three-dimensional earthquake sequence simulations with evolving temperature and pore pressure due to shear heating: Effect of heterogeneous hydraulic diffusivity, *J. Geophys. Res.*, 115(B12), B12314, doi:10.1029/2010JB007780.
- Noda, H. and N. Lapusta (2012), On averaging interface response during dynamic rupture and energy partitioning diagrams for earthquakes, *J. Appl. Mech.*, 79, 031026, doi:10.1115/1.4005964.
- Noda, H. and N. Lapusta (2013), Stable creeping fault segments can become destructive as a result of dynamic weakening, *Nature*, 493, pp. 518-521.
- Noda, H., N. Lapusta, and H. Kanamori (2013), Comparison of average stress drop measures for ruptures with heterogeneous stress change and implications for earthquake physics, *Geophys. J. Int.*, 193, 3, 1691-1712, doi:10.1093/gji/ggt074.
- Perry, S. and N. Lapusta (2016), Reproducing magnitude-invariant stress drops in fault models with thermal pressurization, *International Congress of Theoretical and Applied Mechanics*.

- Perry, S., Lambert, V., and N. Lapusta (2020), Nearly magnitude-invariant stress drops in simulated crack-like earthquake sequences on rate-and-state faults with thermal pressurization of pore fluids. *J. Geophys. Res. Solid Earth*, 125, 3, doi:10.1029/2019JB018597
- Renard, F., C. Voisin, D. Marsan, and J. Schmittbuhl (2006), High resolution 3D laser scanner measurements of a strike-slip fault quantify its morphological anisotropy at all scales, *Geophys. Res. Lett.*, 33(4), L04305.
- Rice, J. R. (1992), Fault Stress States, Pore Pressure Distributions, and the Weakness of the San Andreas Fault, in *Fault Mechanics and Transport Properties in Rocks*, edited by B. Evans and T.-F. Wong, Academic Press, 475-503.
- Rice J.R. (2006), Heating and weakening of faults during earthquake slip, *J. Geophys. Res.*, 111, B05311, doi:10.1029/2005JB004006.
- Sagy, A., E. E. Brodsky, and G. J. Axen (2007), Evolution of fault-surface roughness with slip, *Geology*, 35, 283-286.
- Sato, T., and T. Hirasawa (1973), Body wave spectra from propagating shear cracks, *J. Phys. Earth*, 21, 415-431.
- Shearer, P. M., G. A. Prieto, and E. Hauksson (2006), Comprehensive analysis of earthquake source spectra in southern California, *J. Geophys. Res.*, 111, B06303, doi: 10.1029/2005JB003979.
- Sibson, R. H. (1975), Generation of pseudotachylyte by ancient seismic faulting, *Geophys. J. R. Astron. Soc.*, 43, 775-794.
- Suppe, J. (2007), Absolute fault and upper crustal strength from wedge tapers, *Geology*, 35, 1127-1130.
- Tanikawa, W. and T. Shimamoto (2009), Frictional and transport properties of the Chelungpu fault from shallow borehole data and their correlation with seismic behavior during the 1999 Chi-Chi earthquake. *J. Geophys. Res.*, 114(B1). doi:10.1029/2008JB005750.
- Thomas M. Y., N. Lapusta, H. Noda, and J.-P. Avouac (2014), Quasi-dynamic versus fully-dynamic simulations of earthquakes and aseismic slip with and without enhanced coseismic weakening, *J. Geophys. Res.*, 119, 1986-2004.
- Townend J., and M. D. Zoback (2004), Regional tectonic stress near the San Andreas fault in central and southern California, *Geophys. Res. Lett.*, 31 (15): Art. No. L15S11.
- Trugman, T., and P. M. Shearer (2017), Application of an improved spectral decomposition method to examine earthquake source scaling in Southern California, *J. Geophys. Res.*, 122, 2890-2910, doi: 10.1002/2017JB13971.
- Tullis, T. E. and J. D. Weeks (1986), Constitutive behavior and stability of fictional sliding in granite, *Pure Appl. Geophys.*, 124, 383-414.
- Tullis, T. E. (2015), Mechanisms for friction of rock at earthquake slip rates, in *Treatise on Geophysics (second edition)*, vol. 4, Earthquake Seismology, edited by H. Kanamori, Elsevier, Oxford, 139-159.
- Uchide, T., P. M. Shearer, and K. Imanishi (2014), Stress drop variations among small earthquakes before the 2011 Tohoku-oki, Japan, earthquake and implications for the main shock, *J. Geophys. Res.*, 119, 7164-7174, doi:10.1002/2014JB010943.
- Venkataraman, A., & Kanamori, H. (2004). Observational constraints on the fracture energy of subduction zone earthquakes, *J. Geophys. Res.*, 109(B5), doi: 10.1029/2003JB002549.
- Viesca, R. C., & Garagash, D. I. (2015), Ubiquitous weakening of faults due to thermal pressurization. *Nature Geoscience*, 8(11), 875-879, doi:10.1038/ngeo2554.
- Wang, Y.-R., Y.-Y. Lin, M.-C. Lee, and K.-F. Ma (2011), Fault zone Q structure discovered from the Taiwan Chelungpu Fault Borehole Seismometers Array (TCDPBHS), *Tectonophysics*, 578, 76-86, doi:10.1016/j.tecto.2011.12.027.
- Wesson, R. L., and O. S. Boyd (2007), Stress before and after the 2002 Denali fault earthquake, *Geophys. Res. Lett.*, 34, L07303.

- Wibberley, C. A. J., G. Yielding, and G. Di Toro (2008), Recent advances in the understanding of fault zone structure, in *The Internal Structure of Fault Zones: Implications for Mechanical and Fluid-Flow Properties*, pp. 5–33, Geol. Soc. of London, London.
- Ye, L., T. Lay, H. Kanamori, and K. Koper (2013), Energy Release of the 2013 Mw 8.3 Sea of Okhotsk Earthquake and Deep Slab Stress Heterogeneity, *Science*, 341, 1380-1385.
- Ye, L., T. Lay, H. Kanamori, and L. Rivera (2016a), Rupture Characteristics of Major and Great ($M_w \geq 7$) Megathrust Earthquakes from 1990-2015: 1. Moment Scaling Relationships, *J. Geophys. Res.*, 121, 821-844.
- Ye, L., T. Lay, H. Kanamori and L. Rivera (2016b), Rupture Characteristics of Major and Great ($M_w \geq 7$) Megathrust Earthquakes from 1990-2015: 2. Depth Dependence, *J. Geophys. Res.*, 121, 845-863.
- Ye, L., T. Lay, H., Kanamori, Z. Zhan, and Z. Duputel (2016c), Diverse rupture processes in the 2015 Peru deep earthquake doublet, *Science Advances*.
- Zoback, M.D., S. Hickman, and W. Ellsworth (2007), The role of fault zone drilling, in *Treatise on Geophysics*, vol. 4, Earthquake Seismology, edited by H. Kanamori, Elsevier, Amsterdam.